# Flat-field calibration of CCD detector for Long Trace Profiler

Jonathan L. Kirschman*, Edward E. Domning, Keith D. Franck, Steven C. Irick,
Alastair A. MacDowell, Wayne R. McKinney, Gregory Y. Morrison, Brian V. Smith,
Tony Warwick, Valeriy V. Yashchuk
Lawrence Berkeley National Laboratory, Berkeley, California, USA 94720

## ABSTRACT

The next generation of synchrotrons and free electron lasers requires x-ray optical systems with extremely high-performance, generally, of diffraction limited quality. Fabrication and use of such optics requires highly accurate metrology. In the present paper, we discuss a way to improve the performance of the Long Trace Profiler (LTP), a slope measuring instrument widely used at synchrotron facilities to characterize x-ray optics at high-spatial-wavelengths from approximately 2 mm to 1 m. One of the major sources of LTP systematic error is the detector. For optimal functionality, the detector has to possess the smallest possible pixel size/spacing, a fast method of shuttering, and minimal non-uniformity of pixel-to-pixel photoresponse. While the first two requirements are determined by choice of detector, the non-uniformity of photoresponse of typical detectors such as CCD cameras is around 2-3%. We describe a flat-field calibration setup specially developed for calibration of CCD camera photo-response and dark current with an accuracy of better than 0.5%. Such accuracy is adequate for use of a camera as a detector for an LTP with performance of ~0.1 microradian (rms). We also present the design details of the calibration system and results of calibration of a DALSA CCD camera used for upgrading our LTP-II instrument at the ALS Optical Metrology Laboratory.

**Keywords:** long trace profiler, LTP, LTP detector, camera calibration, flat field source, error reduction, optical metrology

## 1. INTRODUCTION

The long trace profiler (LTP) schematically shown in Fig. 1, is the basic metrology tool for measuring the slope profile of X-ray optics with accuracy on the order of one microradian.[1-5] The design and development of modern high-performance X-ray optical systems requires an LTP with accuracy at sub-microradian levels.[6-10] To be capable of measuring such optics, systematic errors and noise must be suppressed throughout the entire LTP system. A significant amount of error of slope measurement is due to the detector,[11] which in most LTPs consists of a single linear photo-diode array (PDA), or two such arrays in parallel with one used as the sample channel and the other as a reference channel.[5] Compared to an area detector (e.g., area CCD camera), a detector based on a linear array has obvious disadvantages. First, it doesn't allow appropriate alignment of the LTP optics. As a result, the 1D interference pattern recorded with the array often has a significantly perturbed shape, limiting the accuracy of positioning of the pattern. Second, it does not allow for monitoring the curvature of a sample mirror in the sagittal direction. This feature is very important when a toroidal or twisted surface is under investigation. Third, large sagittal size of the beams and poor sagittal resolution of the array LTP detector results in the 'ghost' effect[12] and the systematic error related to the physical difference of the optical paths between the sample and the reference beams.[11,13] Finally, the resolution of a linear array is limited by the pixel width (25 μm for the LTP-II detector) and the resolution of its analog to digital converter (ADC), while a CCD has potentially many more pixels.

In the present work, we describe the results of our recent upgrade of the LTP-II instrument at the ALS optical Metrology laboratory (OML) and provide the detail of the upgrade. We begin by examining the characteristics and performance of the previous LTP detector system, particularly the primary contributions of error and noise to surface slope measurements, (Sec. 2). We can then explore the general steps necessary to achieve greater accuracy with the LTP. Section 3 is devoted to the CCD camera calibration. We then describe and perform evaluations of a specific system recently used to upgrade the LTP at the ALS Optical Metrology laboratory (Sec. 4 and Sec. 5), and finally illustrate the methodology and performance of the system when measuring a high-performance optic to be used on an x-ray beamline (Sec. 6).

*JLKirschman@lbl.gov; tel +1-510-486-4117; fax +1-510-486-7696

Advances in Metrology for X-Ray and EUV Optics II, edited by Lahsen Assoufid, Peter Z. Takacs, Masaru Ohtsuka,
Proc. of SPIE Vol. 6704, 67040J, (2007) · 0277-786X/07/$18 · doi: 10.1117/12.732618

## 2. REQUIREMENTS FOR A DETECTOR / CCD CAMERA

The photo-detector of the LTP is the determining factor for the limit of accuracy to the position of the sample/reference beams and thus determines the limit to the ultimate accuracy for surface slope measurements. The performance of the previous detector and its characteristics leading to systematic errors and noise was studied in previous work.[11] A summary of this work with special attention to factors affecting the choice of an alternative detector is presented below.

The detector previously used in the LTP consisted of two linear photo-diode arrays used to each measure the spatial distribution of either the sample or the reference beam. The effective size of the pixels is specified as 25 μm × 2.5 mm, and readout is performed by a shift-register circuit and converted into digital output by a 16-bit resolution ADC. The contributing factors to error are summarized in Table 1.

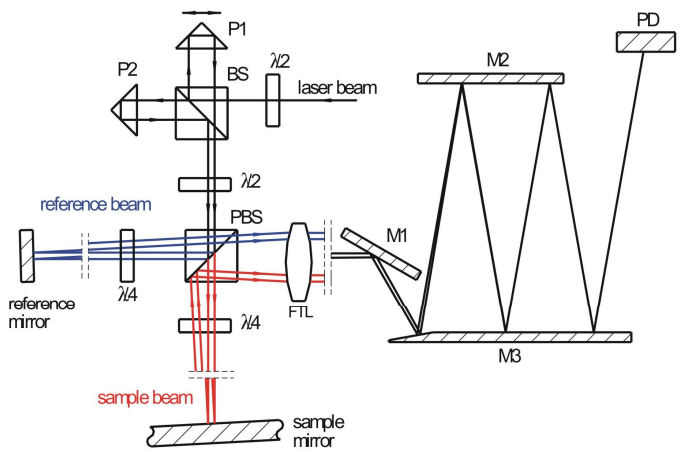


Figure 1: Optical schematic of the LTP at the ALS Optical Metrology Laboratory before modernization. The detector (labeled PD in the figure) is comprised of a beam splitter and two linear photo-diode arrays.

Table 1. LTP-II positioning error due to different sources of noise while using a linear PDA as a detector. $n$ is the number of pixels involved in finding the position of an interference minima on the detector. The last column presents the asymptotic dependences of the errors on $n$. For more details see Ref.[11]

| Noise source | Position error (pixel) at $n = 11$ | Slope error (μrad) | | Asymptotic dependence with n |
|---|---|---|---|---|
| | | $n = 11$ | $n = 23$ | |
| PDA dark signal | $6 \cdot 10^{-4}$ | 0.006 | 0.002 | $\propto n^{-1/2}$ |
| Read-out noise | $2 \cdot 10^{-2}$ | 0.2 | 0.07 | $\propto n^{-1/2}$ |
| ADC resolution (at $2^{10}$ bits) | $2 \cdot 10^{-3}$ | 0.06 | 0.02 | $\propto n^{-1/2}$ |
| PDA photo-response (at 2%) | $3 \cdot 10^{-2}$ | 0.3 | 0.2 | $\propto n^{-1/2}$ |
| Pixel pitch non-uniformity (at 10%) | $3 \cdot 10^{-2}$ | 0.3 | 0.2 | $\propto n^{-1/2}$ |
| Signal shot noise | $2 \cdot 10^{-4}$ | 0.002 | 0.001 | $\propto n^{-3/4}$ |

The primary characteristics of LTP slope error based on a photo-diode array are photo-response non-uniformity, read-out noise, and pixel-pitch non-uniformity.

Photo-response non-uniformity arises from the quality of the CMOS process and results in not only a different photo-response curve between pixels but also non-linear behavior. A typical value for the level of non-uniformity is 2-3%. For the previous LTP photo-diode array, photo-response non-uniformity was found to be about 2.3%.[11] The photo-response of the PDA was also found to be dependent on temperature. To reduce the amount of error, calibration is required to calculate a photo-response gain factor for each individual pixel. In the course of calibration, a dark current offset for

each pixel is also found. Though it is important to note that the dark current can change in various environmental and temperature conditions (see Sec. 3 for further discussion). A simple calibration method is to use a uniform flat-field light source which has uniformity on the level of the desired accuracy of the calibration. One possibility for such a source is an integrating sphere, which generally reaches a level of uniformity of 1%. This light uniformity is not enough even for calibration of a CCD camera with an 8-bit ADC. In Sec. 3, the use of an LED setup for calibration with approximately 0.5% accuracy is presented.

Pixel pitch non-uniformity, like photo-response non-uniformity, is also dependent on the CMOS process in which each pixel is fabricated. This essentially consists of spacing errors between pixels, and intra-pixel sensitivity issues such as varying quantum efficiency across the pixel, wavelength dependence, crosstalk between pixels, and similar effects. Calibration can partially correct for systematic errors due to pixel pitch non-uniformity, and choice of a camera with less pixel spacing and decreased effective pixel size can increase the accuracy of positioning. Of importance also is the number of defective pixels, which can either be "dead" (little or no signal) or "hot" (always saturated). This is also based on the quality of the fabrication and usually factors into the price as well.

Noise and read-out error from the chip and associated electronics is also a significant source of error. This depends largely on the design of the PDA and the associated internal workings. Varying dark current levels also contribute to this factor. It is essential that the reading of each pixel is properly synchronized or shuttered so that all the pixels collect photons for the same duration of time, and that reading is done at a reasonable rate. A fast exposure time is especially useful for the purpose of averaging several frames or PDA readouts for each measured point, which can substantially decrease noise such as that described above and various other effects, such as air convection noise (discussed further in section 5).[14]

Based on the sources of positioning error as listed in Table 1 (for more details, see Ref.[11]), general requirements for an improved detector can be extrapolated. A high amount of pixels and thus small pixel size, plus electronic read-out with low noise, high speed, and a form of shuttering are important traits. Additionally, an ADC converter with 8- or 10-bit resolution is enough to reach accuracies to the goal of 0.1 μrad. Finally, temperature stabilization is necessary to reduce variations in photo-response, lower noise levels, and stabilize the level of dark current. One way of increasing the effective number of pixels and thus suppressing many of the above issues is to use a 2-D CCD to replace the linear arrays. The effective number of pixels in each measurement can be increased substantially by integrating in the sagittal direction. Particularly of importance is that movement of the sample beam can be viewed in the sagittal direction, which is extremely useful when measuring toroidal or twisted surfaces. Also, the beam splitter required to direct the sample and reference beams to each associated PDA can be eliminated and both beams can be read by the same detector.

## 3. CAMERA CALIBRATION

The calibration of a CCD camera is required in order to approach the goal of slope measurements on the order of 0.1 μrad. The method of calibration chosen was to utilize an LED with similar wavelength to that of the LTP beam to generate a flat-field of light. A diagram of the setup is shown in Fig. 2.

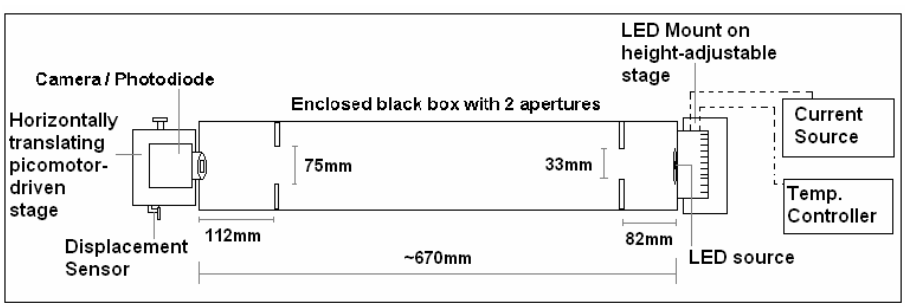


Fig. 2. Flat-field light generation setup based on a current and temperature controlled LED source and a long enclosure. A photodiode was used to check the uniformity of the field.

The LED used to generate the flat field (Luxeon emitter LXHL-PD01) for the calibration apparatus, due to high power dissipation (up to 5 Watts), requires thermal stabilization for temporal stability.[15] It was thus mounted on a laser-diode mount equipped with two thermo-electric coolers rated to provide up to 20 Watts of cooling. This mount was connected to a compatible temperature controller capable of temperature stability of 0.2 mK, set for 23.3°C. The LED current input was controlled with a current driver with specified stability 0.1 mA (setting accuracy ±1mA).

The LED and mount were placed on a height-adjustable platform at one end of a long rectangular metal box (~ 0.67 meters long) with the inside surface painted black. The box contains two apertures to decrease light scattered by the box walls, and the box was enclosed so that all materials on the inside were relatively non-reflective. At the opposite end of the box was the camera, mounted on a picomotor-driven stage capable of horizontal translation with position determined by a displacement transducer.[16] In order to test the temporal stability and spatial uniformity of the flat field light source, a photodiode was mounted in place of the camera. An iris diaphragm with ~0.3 mm open aperture was placed in the front of the photodiode. This photodiode was translated horizontally across the light field over a distance of 10mm in 30 minutes. A variation of the photodiode signal during the motion is a signature of deviation from flatness of the light field, temporal stability of the light intensity, and photodiode efficiency at the same time.

In order to separate spatial non-uniformity from temporal, multiple measurements with the photodiode were averaged and the dependence of non-uniformity on the number, $N$, of measurements averaged was investigated – Fig. 3. The non-uniformity parameter is defined as a variation (RMS) of the measured intensity normalized to the averaged magnitude of the intensity.

The data in Fig. 3 was fit with a simple function: $U(N) = U0 + U1/\sqrt{N}$, where the first term represents the systematic effect due to the repeated spatial variation, independent of averaging, and the second term is due to a random part of the variation. The result of the fit presented as an inset in Fig. 3 indicates that any spatial non-uniformity independent of temporal noise was not detected, $U0 \approx 0.0000$. At the same time, the temporal instability of the light source can be characterized to be better than 0.46%, $U1 \approx 0.0046$. After 16 averages of photodiode translation across 5mm distance (limited due to the moving range of the available translation stage), spatial variance was found to be better than 0.2% standard deviation.

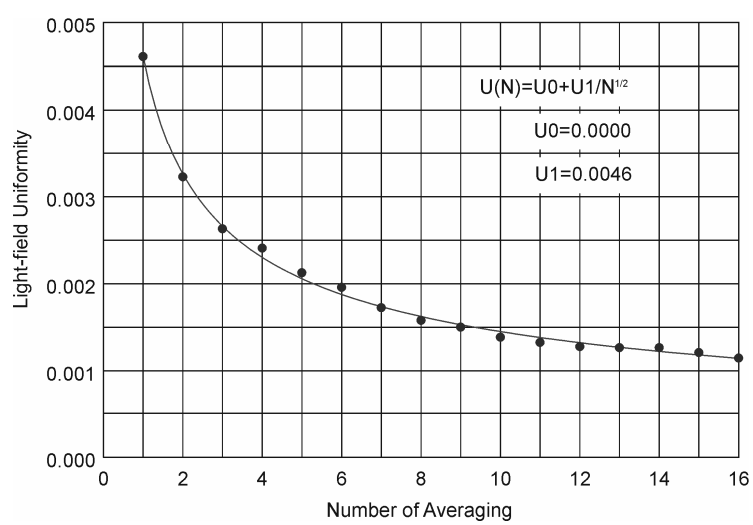


Figure 3: Measure of non-uniformity after averaging multiple measurements with the photodiode. By eliminating temporal noise, the measure of spatial uniformity is improved substantially.

Based upon the considerations in Sec. 2, a camera (Dalsa Pantera SA 4M15[17]) was selected to be calibrated using the system described above and to eventually be mounted on the long trace profiler as an upgrade from the previous detector. The camera used has 2094×2094 pixels with size of a pixel of 7.4 μm×7.4 μm. The camera is capable of

recording up to 16 frames per second, it has an electronic shutter to limit pixel collection times, and an 8-bit ADC. The 8-bit ADC is adequate because the 2-D nature of the camera allows the integration of many pixels to compensate for the lack of resolution; thus, the effective resolution is much greater. Before calibration, the pixel-to-pixel non-uniformity of the camera was found to be on the level of 1.3-1.5% before calibration. Following calibration, pixel-to-pixel non-uniformity was on the level of 0.5%, approaching the limit based upon the resolution of the 8-bit ADC. Additionally, 22 bad pixels were found and, through the software, averaged based on neighboring pixels. The results of the calibration process are shown in Figs. 4 and 5. See Ref.[18] for further detail.

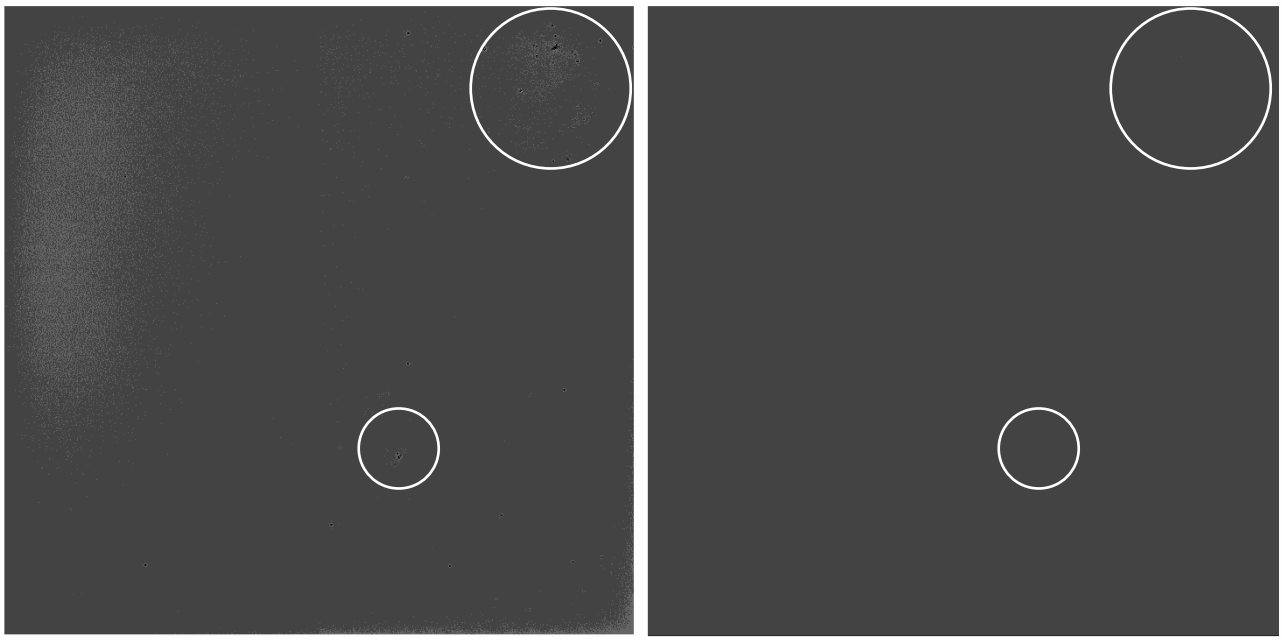

Figure 4: A comparison of an uncorrected image (left) of a flat field illumination of the CCD camera, and the same image (right) after calibration of pixel-to-pixel photo-response non-uniformity is applied (note that contrast has been increased to improve visibility). The white circles indicate areas with concentrations of bad pixels. Additionally, in the uncorrected image, a close inspection reveals a gain difference between the left and right side of the image, due to the dual-tap nature of the camera. The difference in gain is compensated for by the calibration in the image on the right.

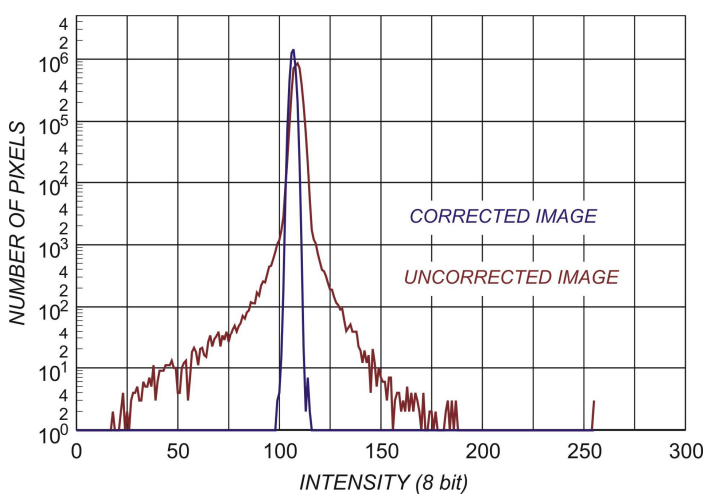


Figure 5: Histograms of the pixel intensities in the uncorrected and corrected images shown in Fig. 4. The logarithmic scale is used to emphasize the contribution of pixels with a large perturbation of efficiency. After correction is applied, the width of the distribution significantly decreases to the inherent limit given by the resolution of the 8-bit camera ADC.

It was also noted in Sec. 2 that temperature stabilization is an important factor in controlling levels of noise, particularly to stabilize dark current levels. The camera was mounted with a thermo-electric cooling element and a heat-sink/fan, along with a temperature controller. This keeps the camera at a temperature (slightly above room temperature to prevent condensation) stable to ~1mK.

## 4. LTP UPGRADE WITH NEW DETECTOR

The new detector, selected based on the requirements in Sec. 2 and calibrated as described in Sec. 3, was used as part of a major upgrade/modernization to the existing LTP in the Optical Metrology Lab at the ALS. The CCD and the temperature control equipment were mounted on the LTP carriage, and a laser beam attenuator (based on two cross-polarizers) with a removable filter was added immediately next to the source laser to prevent the detector pixels from reaching saturation levels. Additional tuning of the drive and motor system, implementing a distance measuring interferometer for location feedback, balancing of the carriage, and installing a new computer were also a part of the modernization process.[19] A picture of the LTP carriage before and after is presented in Fig. 6.

The new detector also required substantial software development in order to acquire image frames from the detector and perform necessary functions such as averaging of multiple frames, applying calibration factors, and finding the centroid of each beam spot to convert to slope. This process is outlined in further detail in Fig. 7.

The boxes in Fig. 7 represent the areas of integration for each beam spot. At the beginning of measurement, a value for the dark current is taken from areas indicated on other parts of the CCD. This compensates partially for the light that leaks into the LTP enclosure. Pixels in each area of interest are then integrated in the sagittal direction to produce an interference picture. The location of each peak is found, and the number of points between the peaks to be used in fitting is established based on a set parameter which takes a fraction of the points depending on the height of each individual peak. After centering the coordinate system, a parabola is fit to the points and a sub-pixel position is found, multiplied by a linear slope conversion factor, and recorded. From the calculation of spot position, we are able to extract the dispersion of the fitted points to be on the level of ~0.0002 $\mu rad^2$ that corresponds to the positioning error of approximately 0.014 μrad. Thus, the fitting algorithm is not a significant contributor to the overall error of the slope trace.

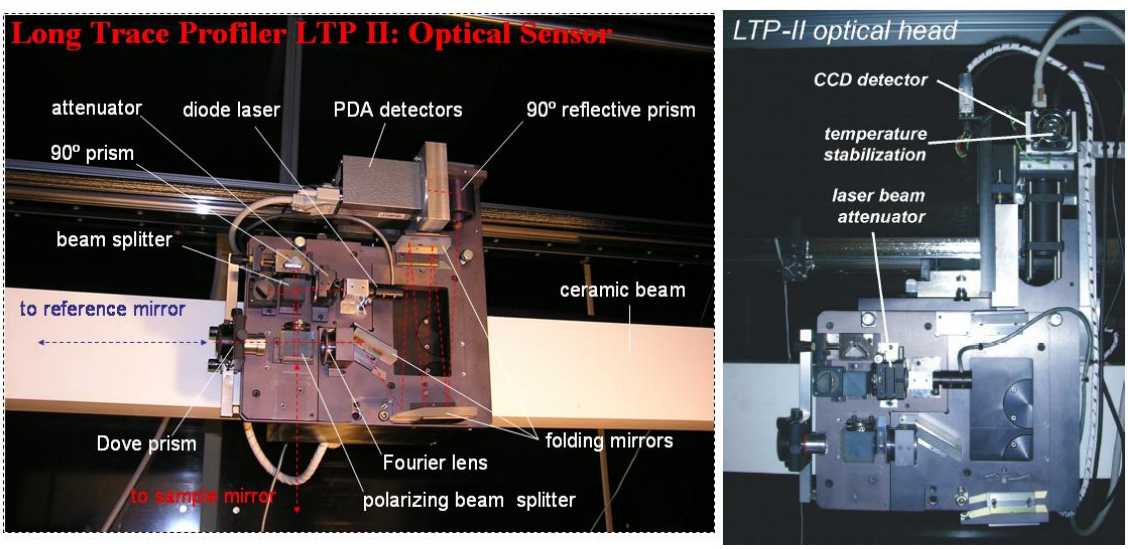


Figure 6: Optical sensor of the LTP before (the left-hand picture) and after (the right-hand picture) upgrade with a new detector system based on a precisely calibrated CCD camera with active temperature stabilization. A new laser beam attenuator was also added to the design to simplify alignment and fine-tune beam intensity.

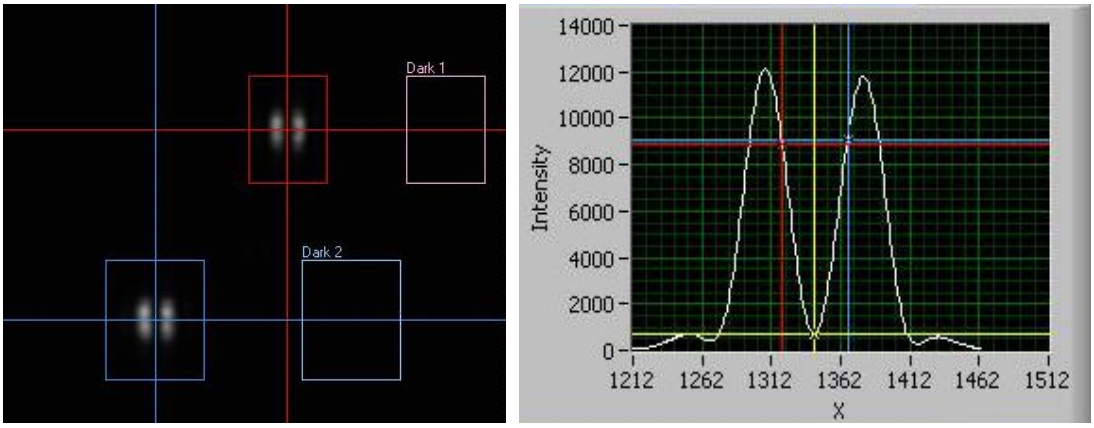


Figure 7: Image from the CCD of sample and reference beams (left) and the corresponding interference picture (right) for the upper (sample) spot. Note that the integrated intensity values have an effective resolution higher than the 8-bit ADC, and that the coordinates for the interference picture are in absolute camera pixels.

Another important factor concerning this upgrade is the choice of motion scheme. The current camera system is capable of gathering a maximum of 16 frames per second, which is adequate for measuring while the carriage is moving (at a speed of about 1 or 2 mm/sec). However, a stop-start scheme of motion, with adequate settling time after a move, was found to be simpler to implement and gave the benefit of allowing the user to take several camera frames for each point along the mirror trace. It has also been shown that taking measurements while the carriage is in motion can yield increased noise due to varying accelerations and movement fluctuations of the carriage.[20]

## 5. METHODS AND TECHNIQUES WITH 2D DETECTORS

With the implementation of the new 2-D detector, the capabilities of the LTP are expanded beyond the previous operation. The expanded field of view (see Fig. 7) allows us to view the entire beam spot for the first time. Additionally, the position of these spots can be can be modified by tilting the surface under test (SUT). With the capability of viewing the entire beam spot instead of a single cross-section, it is possible to adjust the alignment of the beam in relation to the rest of the LTP optics (especially to compensate for off-axis tilt of the beam). The extended field of view in the vertical direction also allows easier adjustment of the SUT to focus on the detector.

Equal spatial resolution in both tangential and sagittal directions, intrinsic to an area CCD detector, allows in principle for a more precise beam position location due to the significantly larger number of pixels involved in fitting. A common difficulty in measuring toroidal or twisted surfaces in the LTP is the defocus of the beam. While alignment can be useful in reducing this, it is sometimes difficult to get enough signal amplitude with a linear detector. However, since the area of pixels to be integrated can be varied, a 2D detector allows the operator to select a large portion or the entire spot in order to obtain a better measurement.

Averaging of several camera frames at each point of measurement is useful for decreasing noise. A particular source of noise in LTP instruments is due to air convection currents. A typical measurement of the LTP at the ALS OML is done with 10 frames averaged over a second, which roughly corresponds to the frequency of air convection noise[14] and reduces these effects by a factor of approximately 3.

A method that has become possible with the implementation of a 2-D detector is to sagittally tilt a mirror under test in order to change the path of the LTP sample beam (see also Ref.[21]) through the glass optics of the instrument. A sagittal tilt would lead to a shift of the measured trace in the sagittal direction in the field of view of the LTP 2D detector. The total available range of tilts is determined by the size of the aperture of the CCD camera used. The range of the upgraded LTP in both tangential and sagittal directions is approximately 5 mrad. Therefore, tilting with a step of ~50 μrad would provide the possibility for a large enough number of independent measurements. This method was found to be especially effective in optics where the specification of the mirror is close to or below the level of noise and

systematic error for the instrument. One such optic which was measured with the upgraded LTP at the ALS OML is described in Sec. 6.

## 6. LTP PERFORMANCE FOLLOWING UPGRADE

The first metrology work[22] with the updated LTP was performed with a super polished grating substrate with a spherical radius of ~18.7 m, fabricated by InSync Inc. for the MERLIN project.[6] The rms slope variation for the substrate was originally specified to be <0.25 μrad. However, due to fabrication problems related to the difficulty of adequate metrology, the specification was reduced to the level of <0.5 μrad. The measurement performed at the OML indicates a slope variation of <0.37 μrad for the central part of the substrate. This was found by calculating the contribution of systematic error and noise from the results of the averaging technique described in Sec. 5.

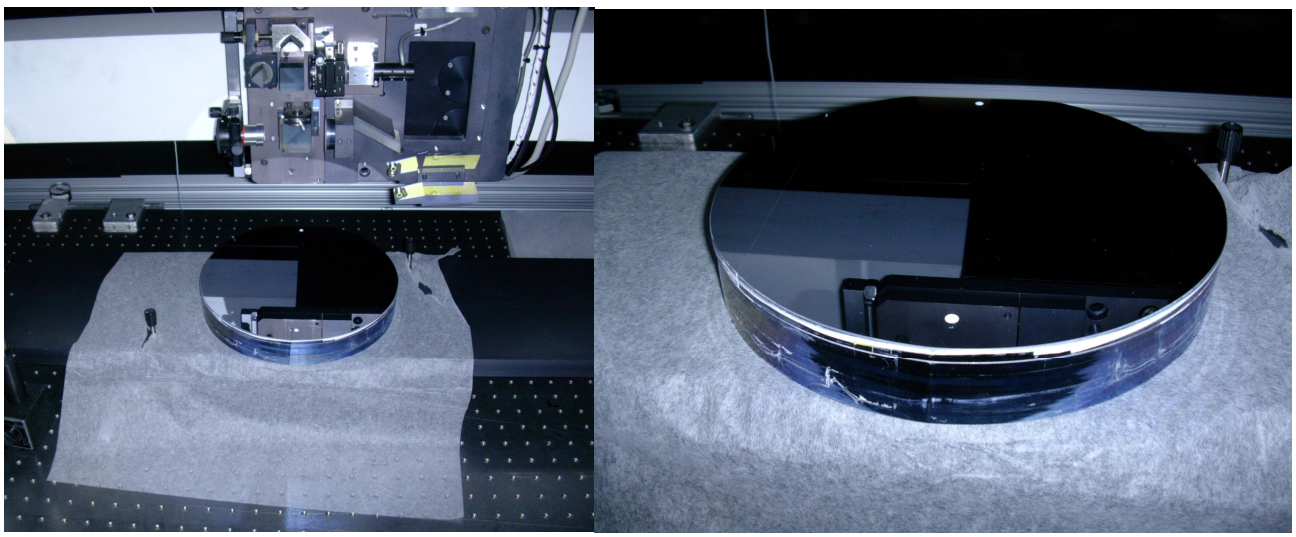

Figure 8: Super polished grating substrate with specification of <0.5 μrad (rms) slope deviation set to be measured on the upgraded LTP.

Using the data from the multiple tangential scans (with and without sagittally tilting), the RMS variation of each portion of the substrate along with the contribution of random noise and some systematic errors was calculated using the following:

$$\begin{aligned} \sigma_r^2 + \sigma_m^2 &= \hat{\sigma}_1^2, \\ \sigma_r^2 / N + \sigma_m^2 &= \hat{\sigma}_N^2, \end{aligned} \tag{1}$$

where $\hat{\sigma}_1$ is the RMS variation for one measurement averaged over the RMS variations of all individual measurements, $\hat{\sigma}_N$ is the RMS variation of a slope trace found by averaging all N measurements, $\sigma_r$ is the RMS variation due to the random noise and systematic error, which can be averaged out), and $\sigma_m$ is RMS variation due to the mirror surface slope variation and the systematic error (mostly this is the low spatial frequency systematic error) that cannot be averaged with the described method and therefore, cannot be separated from the mirror surface slope error.

Using the above calculation with 6 scans of the same slope trace (see Fig. 9 for slope and height of the optic), we were able to ascertain the surface variation of the grating blank as <0.37 μrad (rms) despite an original, single slope trace having a variation on the level of 0.64 μrad. With this method, the higher-spatial-frequency systematic errors of the LTP optics are significantly suppressed. This capability is only possible with a 2-D detector, which to our knowledge is not

in use in most of the LTP instruments around the world. At the time of this writing, our accuracy of LTP measurements after modernization is on the level of ~0.3 μrad for very curved mirrors.

## 7. CONCLUSION

We have considered the problems of the LTP instrument related to the photo-detector, and have established that it is one of the most important factors in determining the ultimate accuracy of LTP slope measurements. These problems originate mostly in the properties of the fabrication process and the characteristics of the detector itself, and it has been found that the pixel-to-pixel photoresponse non-uniformity in particular is a major factor in limiting instrument accuracy. A 2-D CCD detector allows an increased number of pixels to be involved in measurements, and also allows measurement of the slope in the sagittal direction.

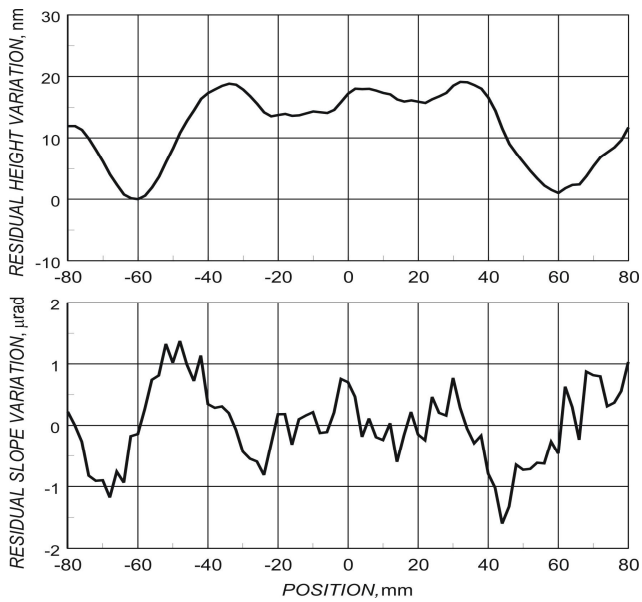


Figure. 9: Super polished grating substrate slope and height profiles from the LTP. Note the symmetrical nature of the profile, which is characteristic of the polishing process.

Much of the contribution of systematic errors can be suppressed with appropriate calibration. A setup for calibration using a uniform flat-field source was designed and implemented with spatial uniformity of ~0.2%, and a particular camera based on the requirements established by analysis of the old detector was thermally stabilized and calibrated. Calibration resulted in a reduction of photoresponse non-uniformity from 1.3% to less than 0.5%.

The LTP at the ALS OML was upgraded with the new detector, which resulted in improved performance and a change from a continuous motion scheme for the LTP carriage to stop-start motion. Additionally, the 2-D nature of the detector allowed a number of techniques and methods to be implemented. Both sample and reference beams are on the same detector, and control over the intensity and alignment of the beams was improved. Averaging of multiple frames helps to suppress air convection noise. Finally, a method for averaging out additional systematic errors is possible, based on tilting the surface under test to reflect to a different location on the CCD and thus changing the optical path of the beam. This approach was successfully utilized in performing metrology on a high-quality grating substrate. Further details on the upgrade process of the LTP at the ALS OML can be found in Refs.[19,21,22] and are also available upon request.

## ACKNOWLEDGEMENTS

The authors are grateful Howard Padmore and Frank Siewert for extremely useful discussions. This work was supported by the U. S. Department of Energy under contract number DE-AC02-05CH11231.

## DISCLAIMER

Certain commercial equipment, instruments, software, or materials are identified in this document. Such identification does not imply recommendation or endorsement by the US Department of Energy, LBNL or ALS nor does it imply that the products identified are necessarily the best available for the purpose.

## REFERENCES

1 E. L. Church, P. Z. Takacs, *Use of an optical profiling instrument for the measurement of the figure and finish of optical quality surfaces*, Wear, 109, 241-57, (1986).
2 P. Z. Takacs, Shinan Qian, J. Colbert, *Design of a long trace surface profiler*, Proceedings of SPIE 749 (1987), 59-64.
3 P. Z. Takacs, S. K. Feng, E. L. Church, Shinan Qian, W-M. Liu, *Long trace profile measurements on cylindrical aspheres*, Proceedings of SPIE , 966 (1989), 354-64.
4 S. C. Irick. W. R. McKinney, *Advancements in one-dimensional profiling with a long trace profiler*, Proceedings of SPIE, 1720 (1992), 162-8.
5 S. C. Irick, W. R. McKinney, D. L. Lunt, P. Z. Takacs, Using a straightness reference in obtaining more accurate surface profiles from a long trace profiler (for synchrotron optics), Rev. Sci. Instrum., 63(1) , 1436-8 (1992).
6 Beamline 4.0.1: High-Resolution Spectroscopy of Complex Materials (MERLIN); www-als.lbl.gov/als/techspecs/bl4.0.1.html.
7 D. Krämer, E. Jeschke, W. Eberhardt, "The BESSY Soft X-ray Free Electron Laser – Technical Design Report, March 2004, Berlin; www.bessy.de/publicRelations/publications.
8 R. Follath, "Design of FEL-Beamlines for Short Pulse, High Resolution and High Power Density," AIP Conference Proceedings **879** (2007).
9 A. Aghababyan , et al., "The European X-Ray Free-Electron Laser - Technical Design Report," Editors: M. Altarelli, et. al.; http://xfel.desy.de/tdr/index_eng.html.
10 National Synchrotron Light Source II, www.bnl.gov/nsls2.
11 V. V. Yashchuk, "Positioning Errors of Pencil-beam Interferometers for Long Trace Profilers," Proc. SPIE 6317, 63170A (2006).
12 V. V. Yashchuk, S. C. Irick, and A. A. MacDowell, "Elimination of 'ghost'-effect-related systematic errors in metrology of x-ray optics with a long trace profiler," Proc. SPIE 5858, 58580X (2005).
13 V. V. Yashchuk, W. R. McKinney, T. Warwick, T. Noll, F. Siewert, T. Zeschke, R. D. Geckeler, "Proposal for a Universal Test Mirror for Characterization of Slope Measuring Instruments," SPIE Proc. **6704**-09 (2007) – this volume.
14 V.V. Yashchuk, S.C. Irick, A.A. MacDowell, W.R. McKinney, and P.Z. Takacs, "Air convection noise of pencil-beam interferometer for long trace profiler," Proc. SPIE **6317**, 63170D (2006).
15 Luxeom application brief AB23: "Thermal Design Considerations for Luxeon 5 Watt Power Light Sources" (http://www.lumileds.com/pdfs/AB05.PDF).
16 J. L. Kirschman, R.S. Celestre, S.C. Irick, A.A. MacDowell, W.R. McKinney, T. Warwick, V.V. Yashchuk, "Characterization of Displacement Sensors to be used with KB Mirrors," ALS Beamline Note, LSBL 791, (2006).
17 Pantera SA 4M15 Area Scan Camera product specifications sheet 2 (http://vfm.dalsa.com/catalog/4M15_product_sheet_00182-06.pdf).
18 J. L. Kirschman, B.V. Smith, E.E. Domning, W.R. McKinney, S.C. Irick, A.A. MacDowell, T. Warwick, V.V. Yashchuk, "Camera Calibration with LED Source for Long Trace Profiler," ALS Beamline Note, LSBL-801 (2006).

19 E. E. Domning, K.D. Franck, J.L. Kirschman, A. A. MacDowell, W.R. McKinney, G.Y. Morrison, B.V. Smith, T. Warwick, V.V. Yashchuk, Upgrade of the Long Trace Profiler LTP-II. Part 1: Modification and Tuning of the LTP-II Translation System, ALS Beamline Note, LSBL-832, (2006).
20 J. L. Kirschman, E.E. Domning, S.C. Irick, A.A. McDowell, G.Y. Morrison, B.V. Smith, V.V. Yashchuk, Characterization of Linear Translation Stage for Developmental Long Trace Profiler, ALS Beamline Note, LSBL-798 (2006).
21 J. L. Kirschman, W. R. McKinney, V. V. Yashchuk, "Upgrade of the Long Trace Profiler LTP-II. Part 3: A New Method for Suppression of the LTP Systematic Error," ALS Beamline Note, LSBL-829, (2006).
22 J. L. Kirschman, W.R. McKinney, V.V. Yashchuk, "Upgrade of the Long Trace Profiler LTP-II. Part 4: LTP Metrology of 18.7-m Grating Substrate for the MERLIN Project," ALS Beamline Note, LSBL-830, (2006).